Finger crease pattern recognition using Legendre moments and principal component analysis

Rongfang Luo (罗荣芳)[1,2] and Tusheng Lin (林土胜)[1]

[1]*School of Electronics and Information Engineering, South China University of Technology, Guangzhou 510640*

[2]*Faculty of Construction, Guangdong University of Technology, Guangzhou 510640*

Received April 29, 2006

The finger joint lines defined as finger creases and its distribution can identify a person. In this paper, we propose a new finger crease pattern recognition method based on Legendre moments and principal component analysis (PCA). After obtaining the region of interest (ROI) for each finger image in the pre-processing stage, Legendre moments under Radon transform are applied to construct a moment feature matrix from the ROI, which greatly decreases the dimensionality of ROI and can represent principal components of the finger creases quite well. Then, an approach to finger crease pattern recognition is designed based on Karhunen-Loeve (K-L) transform. The method applies PCA to a moment feature matrix rather than the original image matrix to achieve the feature vector. The proposed method has been tested on a database of 824 images from 103 individuals using the nearest neighbor classifier. The accuracy up to 98.584% has been obtained when using 4 samples per class for training. The experimental results demonstrate that our proposed approach is feasible and effective in biometrics.

OCIS codes: 100.5010, 100.2000, 100.2960.

Biometrics is defined as the measurable physiological and/or behavioral characteristics used to verify the true identity of an individual. It uses image processing and pattern recognition technologies to identify the personal features. Recently, issues on palmprint identification, face recognition, and iris-based verification have been studied extensively, which results in successful development of biometric systems for commercial applications. However, each of them having its own advantages and disadvantages, according to user acceptance, cost, performance, etc.[1]. No single biometric is expected to effectively meet the requirements of all applications[1]. Therefore, to develop new individual characteristics for biometric techniques becomes an important task.

There are some features on the front surface of a finger, called the finger crease lines, which are very salient pattern after the fingerprint, and thought to be stable and different for each individual[2]. However, insufficient attention has been paid to finger crease as a biometric characteristic. So far, although many verification technologies using biometric features of palms were developed recently[3−6], there are few literatures about the finger crease as biometric feature[2,7,8]. From all biometric techniques, finger crease is considered to achieve medium security, but with several advantages compared with the other physical characteristics[2]: high processing speed, resistance to noise, low system cost. All these encourage us to employ the finger crease for personal recognition. In this paper, a new finger crease recognition approach based on Legendre moments and Karhunen-Loeve (K-L) transform is presented.

When finger images are captured, the position, direction, and stretching degree of a hand may vary from time to time. Therefore, even images from the same finger may have a little rotation and shift. Furthermore, the sizes of fingers are different from one another. Hence finger images should be orientated and normalized before feature extraction and matching.

Given a finger image of 256 gray levels, as shown in Fig. 1(a). It is important to define a coordinate system to align different finger images for matching. To extract the central rectangular window part of a finger, we use the central/principal axes of the fingers contour region to determine a coordinate system (see Figs. 2(b) and (c)). The basic steps of finger alignment are defined as follows.

1) Use a threshold to convert from the original gray level image into a binary image. The finger images of 256 gray levels are acquired from a platform scanner. The image-thresholding operation is to binarize the gray images to obtain the binary finger-shape images. In this step, the histogram of gray images is analyzed as shown in Fig. 1(b) to determine a threshold value. The binary image is shown in Fig. 2(a).

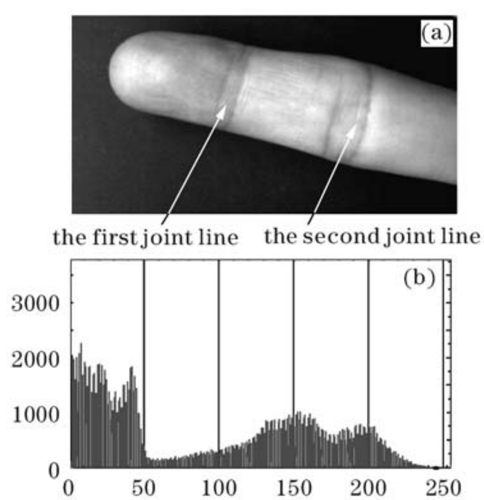

Fig. 1. (a) Original image and (b) the corresponding histogram diagram.

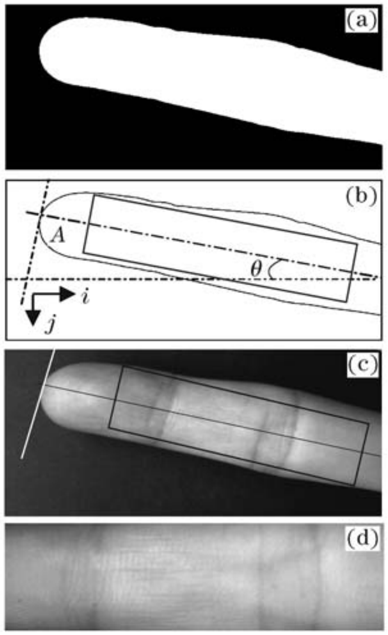

Fig. 2. The main steps of pre-processing. (a) Binary image; (b) deciding a coordinate system; (c) extracting the rectangular part as a subimage; (d) pre-processed result.

2) Calculate moments of two-dimensional (2D) binary image functions $f(x, y)$. For a 2D digital image $f(x, y)$, the moment of order $(p+q)$ is defined as

$$m_{pq} = \sum_x \sum_y x^p y^q f(x, y), \quad p, q = 0, 1, \tag{1}$$

the corresponding central moments is defined as

$$\mu_{pq} = \sum_x \sum_y (x - \bar{x})^p (y - \bar{y})^q f(x, y), \quad p, q = 0, 1, 2, \tag{2}$$

where $\bar{x} = \frac{m_{10}}{m_{00}}$ and $\bar{y} = \frac{m_{01}}{m_{00}}$.

3) Calculate the angle θ between a central axis and the horizontal i-axis, as shown in Fig. 2(b). The angle θ may be obtained from

$$\tan 2\theta = \frac{2\mu_{11}}{\mu_{20} - \mu_{02}}. \tag{3}$$

The central line of region in the finger contour constitutes the x-axis of the finger coordinate system and make a line through A point perpendicular to x-axis, to determine y-axis and the origin of the coordinate system (see Fig. 2(b)). This coordinate system can align different finger images. After obtaining the x-axis of image, rotate the image to make the x-axis on the horizontal direction. Figure 2(c) shows the original image and coordination system decided. The region of interest (ROI) is extracted from the finger images based on the coordinate system. The ROI in this paper is defined in a rectangular shape after the correction of orientation, which includes the first joint lines and second joint lines in the finger image. Then the ROI is converted to a fixed size (80×320 pixels) so that all of the finger images conform to a same size (see Fig. 2(d)).

An important issue in finger crease recognition is to extract crease features that can discriminate an individual from the other. In this paper, we take the invariant feature vector extracted from finger images for finger crease feature. In order to get the feature vector, we propose a feature extraction scheme. Extracting feature vectors from ROI of the finger image is composed of two steps. Firstly, Radon transform is used to project the ROI to one-dimensional (1D) space at different directions, and then to calculate the kth-order Legendre moments for all the projection angles to form $m \times n$ moment feature matrix. Secondly, the feature vectors are created by applying principal component analysis (PCA), also known as K-L transform, to above feature matrix. In the following, we will present the details of each step.

Radon transform, which has been widely discussed and applied in image processing and pattern recognition[9−11], represents an image as a collection of projections along various directions. The Radon transform of a 2D function $f(x, y)$ is defined as

$$R(t, \theta) = \iint_D f(x, y)\delta[t - (x\cos\theta + y\sin\theta)]\mathrm{d}x\mathrm{d}y, \tag{4}$$

where $\delta(x) = \begin{cases} 1 & x = 0 \\ 0 & x \neq 0 \end{cases}$.

The function $R(t, \theta) \in L^2([-1, 1] \times [0, 2\pi])$ is defined for each pair (t, θ) as the integral of f over a line at angle θ with the x-axis and at radial distance t away from the origin.

Let $H_i^{(k)}(\theta)$ denote the kth-order Legendre moment of $R_i(t, \theta)$ for each fixed θ. That is

$$H_i^k(\theta) = \int_{-1}^{1} R_i(t, \theta) P_k(t)\mathrm{d}t, \tag{5}$$

where the function $P_k(x)$ is the kth-order normalized Legendre polynomial over $[-1, 1]$ defined by

$$P_n(x) = \sum_{k=0}^{n} (-1)^{(n-k)/2} \frac{1}{2^n} \frac{(n+k)!x^k}{(\frac{n-k}{2})!(\frac{n+k}{2})!k!}.$$

In addition, the orthogonal moment of $f(x, y)$ is defined as

$$L_{pq} = \frac{(2p+1)(2q+1)}{4} \int_{-1}^{1}\int_{-1}^{1} f(x, y) P_p(x) P_q(y)\mathrm{d}x\mathrm{d}y. \tag{6}$$

In fact, the kth orthogonal moment $H_i^{(k)}(\theta)$ of $R_i(t, \theta)$ is a linear combination of the orthogonal moment L_{pq} of $f(x, y)$ of order $p + q \leq k$.

The corresponding feature matrix is formed as[12]

$$H = [H_0^i \quad H_1^i \quad \cdots \quad H_{n-1}^i], \tag{7}$$

where $H_{n-1}^i = [H_{n-1}^0 \quad H_{n-1}^1 \quad \cdots \quad H_{n-1}^{m-1}]^{\mathrm{T}}$. Because the main feature of finger creases is vertical wrinkle, the Radon transform for the ROI is computed at angles from 0° to 180° with 30° increments, that is $n = 7$; $m \leq 11$, which is explained later.

H contains all the moments of $R_i(t, \theta)$, and provides complete orthogonal decomposition of $R_i(t, \theta)$, therefore, it can represent the principal component of ROI quite well.

PCA is a powerful technique for reducing a large set of correlated variables to a smaller number of uncorrelated components. It has been applied extensively for both feature extraction, pattern recognition[6,13] and other fields[14].

Let the training samples of the finger crease images be $\boldsymbol{x}_1$, $\boldsymbol{x}_2$, $\cdots$, $\boldsymbol{x}_M$, where M is the number of images in the training set. The mean vector of the training set is defined by

$$\boldsymbol{m} = \frac{1}{M}\sum_{i=1}^{M}\boldsymbol{x}_i. \tag{8}$$

The covariance matrix, $\boldsymbol{C}_x$, of $\{\boldsymbol{x}_i\}$ can be approximated by

$$\boldsymbol{C}_x = \frac{1}{M}\sum_{i=1}^{M}(\boldsymbol{x}_i - \boldsymbol{m})(\boldsymbol{x}_i - \boldsymbol{m})^{\mathrm{T}} = \frac{1}{M}\boldsymbol{X}\boldsymbol{X}^{\mathrm{T}}, \tag{9}$$

where the matrix $\boldsymbol{X} = [\boldsymbol{x}_1 - \boldsymbol{m}, \boldsymbol{x}_2 - \boldsymbol{m}, \cdots, \boldsymbol{x}_M - \boldsymbol{m}]$.

In the proposed method, $\boldsymbol{x}_i$ represents a dimensional vector whose length equals the number of elements for feature matrix H rather than that of the finger image pixels. In practice, the maximal size of matrix of moment feature is 11×7. The length K of the vector $\boldsymbol{x}_i$ is relatively small. Thus, the eigenvectors and eigenvalues of matrix $\boldsymbol{C}_x$ ($\boldsymbol{C}_x \in \Re^{K\times K}$) are much easier to calculate.

It is well known that the following formula is satisfied for the matrix $\boldsymbol{C}_x$:

$$\boldsymbol{C}_x\boldsymbol{u}_i = \lambda_i\boldsymbol{u}_i, \tag{10}$$

where $\boldsymbol{u}_i$ refers to the eigenvector of the matrix $\boldsymbol{C}_x$, and λ_i is the correlative eigenvalue of matrix $\boldsymbol{C}_x$.

The eigenvector $\boldsymbol{u}_i$ corresponding to the eigenvalue λ_i spans the base of the sought subspace. Each feature matrix H of original subimage can be projected into this subspace as

$$\boldsymbol{y} = U^{\mathrm{T}}(\boldsymbol{x} - \boldsymbol{m}), \tag{11}$$

where $U = [\boldsymbol{u}_i, i = 1, \cdots, K]$ denotes the transformed matrix corresponding to $\boldsymbol{u}_i$ which corresponds to the original finger images and spans an algebraic subspace called unitary eigenspace of the training set. However, the theory of PCA states that it does not need to choose all of the eigenvectors as the base vectors and just those corresponding to the largest eigenvalues can represent the characteristic of the training set quite well. Then the U_q significant eigenvectors with the largest associated eigenvalues are selected to be the components of the eigenpace ($U_q = [\boldsymbol{u}_i^q, i = 1, \cdots, M_q]$), which can span an M_q dimensional subspace of all possible feature matrices for finger subimages. Equation (11) is transformed as

$$\boldsymbol{y} = U_q^{\mathrm{T}}(\boldsymbol{x} - \boldsymbol{m}), \tag{12}$$

where the weight of the projection $\boldsymbol{y}$ ($\boldsymbol{y} \in \Re^{M_q\times 1}$) refers to the feature vector of each person, and M_q is called the feature length.

Finger images were collected in our laboratory from 103 people using our self-designed capture device, and the tested images contained 8 images per finger from 103 individuals for a total of 824 finger images. The ROI used in the experiments were of the size 80×320 with 256 gray levels and 8 bits per pixel after pre-processing. A nearest neighbor classifier is used to verify the validity of our approach.

The weighted Euclidean distance is used to measure the similarity between these two features[13],

$$d_j = \sum_{i=1}^{N}\frac{(\boldsymbol{y}(i) - \boldsymbol{y}_j(i))^2}{\sigma_j^2}, \tag{13}$$

where $\boldsymbol{y}$ is the feature vector of the unknown finger crease pattern, $\boldsymbol{y}_j$ and σ_j denote the jth feature and its standard deviation, and N is the feature length.

Hence, the matching criterion is given by: If $d_j = \min(d_i)$, $i = 1, 2, \cdots, L$, then $\boldsymbol{y}$ belongs to jth person (L is the number of individuals).

Four kinds of experiment schemes were designed as follows: one (two, three, or four) sample(s) of each person was randomly selected for training, and the other samples were used for identification respectively. During the experiments, the features were extracted by using the proposed method with lengths 5, 10, 15, 20, 30 and 50. Based on these schemes, the matching was separately conducted, and the results are shown in Fig. 3. As Fig. 3 shows, the more samples are trained, the better result will be generated. A good performance of recognition was achieved with feature length of 15, and longer feature length cannot lead to a higher recognition rate. Up to 98.584% of the 412 samples are classified correctly by using four-sample scheme, which demonstrates the effectiveness of our method.

The answer to the question about the satisfactory order of Legendre moments can be obtained by experiments in which the recognition results are analyzed as a function of the order of Legendre moments (i.e. the rows of feature matrix). Figure 4 depicts the results of the experiments, and it shows good performance of recognition when the order of Legendre moments is 11. With increasing the power of $P_k(x)$ (i.e. the order of Legendre moments), the performance of recognition cannot be further improved. According to the results, we choose 11 as the final m (i.e. the rows of feature matrix) value.

In this paper, the method based on finger creases is developed for personal recognition by using Legendre moments and PCA algorithm, which overcomes the drawbacks existing in traditional PCA technique whose covariance matrix is in a high-dimensional space. The

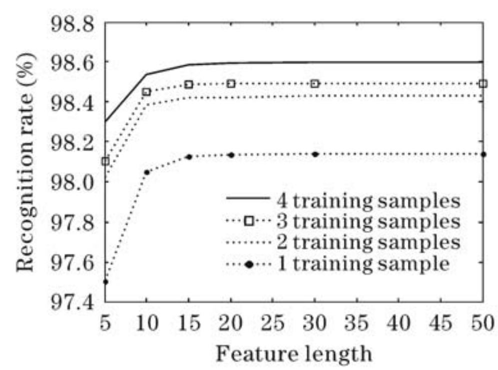

Fig. 3. Recognition rate of different numbers of training samples and feature lengths.

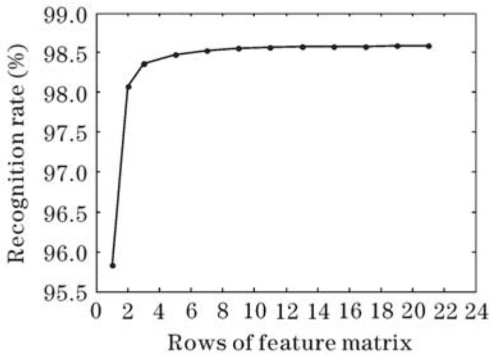

Fig. 4. Recognition rate of different orders of Legendre moments (rows of feature matrix).

proposed approach can directly compute the eigenvectors and eigenvalues of covariance matrix. To assess the efficiency of our method, the weighted Euclidean distance classifier is applied. A correct recognition rate of up to 98.584% can be obtained in our database of 824 images from 103 different persons. The experimental results illustrate the effectiveness of finger creases on the inner side of the fingers as a biometric.

The finger crease as a relative new biometric feature for personal authentication is an important complement to the existing biometric technology, which has the advantage that feature pattern of it is much simpler than many kinds of biometrics such as fingerprint, palmprint, and face. Moreover, finger creases can be obtained in low resolution and low contrast images.

This work was supported by the National Natural Science Foundation of China (No. 60472067) and the Guangdong Provincial Natural Science Foundation for Program of Research Team (No. 04205783). R. Luo's e-mail address is luorfang@163.com.

References

1. A. K. Jain, A. Ross, and S. Prabhakar, IEEE Trans. Circ. Syst. Video Technol. **14,** 4 (2004).
2. M. Takeda, S. Uatoshi, K. Hiramatsu, and T. Matsunami, in *Proceeding of 10th International Conference on Pattern Recognition* 761 (1990).
3. X. Wu, D. Zhang, and K. Wang, IEEE Trans. Syst. Man, Cybern. A **36,** 978 (2006).
4. D. Zhang, W.-K. Kong, J. You, and M. Wong, IEEE Trans. Patt. Anal. Machine Intell. **25,** 1041 (2003).
5. C.-L. Lin, T. C. Chuang, and K.-C. Fan, Pattern Recognition **38,** 2639 (2005).
6. T. Connie, A. T. B. Jin, M. G. K. Ong, and D. N. C. Ling, Image and Vision Computing **23,** 501 (2005).
7. D. G. Joshi, Y. V. Rao, S. Kar, V. Kumar, and R. Kumar, Pattern Recognition **31,** 15 (1998).
8. J. Doi and M. Yamanaka, IEEE Trans. Instrum. Meas. **54,** 2213 (2005).
9. P. Cui, J. Li, Q. Pan, and H. Zhang, Pattern Recognition Letters **27,** 408 (2006).
10. J. S. Seo, J. Haitsma, T. Kalker, and C. D. Yoo, Signal Processing: Image Communication **19,** 325 (2004).
11. E. Magli, G. Olmo, and L. L. Presti, Signal Processing **73,** 277 (1999).
12. P. Milanfar, W. C. Karl, and A. S. Willsky, IEEE Trans. Image Processing **5,** 459 (1996).
13. G. Lu, D. Zhang, and K. Wang, Pattern Recognition Letters **24,** 1463 (2003).
14. Y. Wang and H. Xu, Chin. Opt. Lett. **3,** 725 (2005).